Earth, Planets and Space

EXPRESS LETTER

Open Access

How variable are Birkeland currents?

Johnathan K. Burchill[1*]

Abstract

I address the problem of estimating the time-rate-of-change of high-latitude Birkeland currents by using a string-of-pearls formation of satellites. Space series are calculated by linear interpolation of measurements made at the revisit times of the satellites. A lower bound on the total time derivative can be estimated as a function of distance along the orbit. Space series of the vertical component of electric current density, used as a proxy for field-aligned (Birkeland) current density at high latitude, are estimated from the along-track spatial derivative of Swarm magnetic field measurements residual to the CHAOS-7 internal field model. The results reveal non-negligible total time derivatives over periods shorter than 2 mins. Auroral Birkeland current densities derived from single-satellite traversals of magnetic field gradients can change dramatically in the time it takes a single satellite to cross a large-scale current system. In one example, during an overflight by the Swarm satellites of the THEMIS Fort Yukon all-sky imager on 1 December 2013, the vertical current density poleward of a visually quiescent auroral arc changes from $\sim 0.3\ \mu$ A/m^2 upward to $\sim 1.0\ \mu$ A/m^2 downward in 13.7 s (corresponding to an along-track separation of Swarm A and B of 104 km). The variability of Auroral Birkeland currents, between 25 November 2013 and 31 December 2013, as estimated by the median of $|dj_z/dt|$, reaches 15 nA/m^2/s in the northern dayside auroral zone and exceeds 30 nA/m^2/s in the pre-noon sector of the southern hemisphere.

Keywords Ionosphere, Magnetic field, Electric current density, Swarm, Space-time series

*Correspondence:
Johnathan K. Burchill
jkburchi@ucalgary.ca
Full list of author information is available at the end of the article

Graphic Abstract

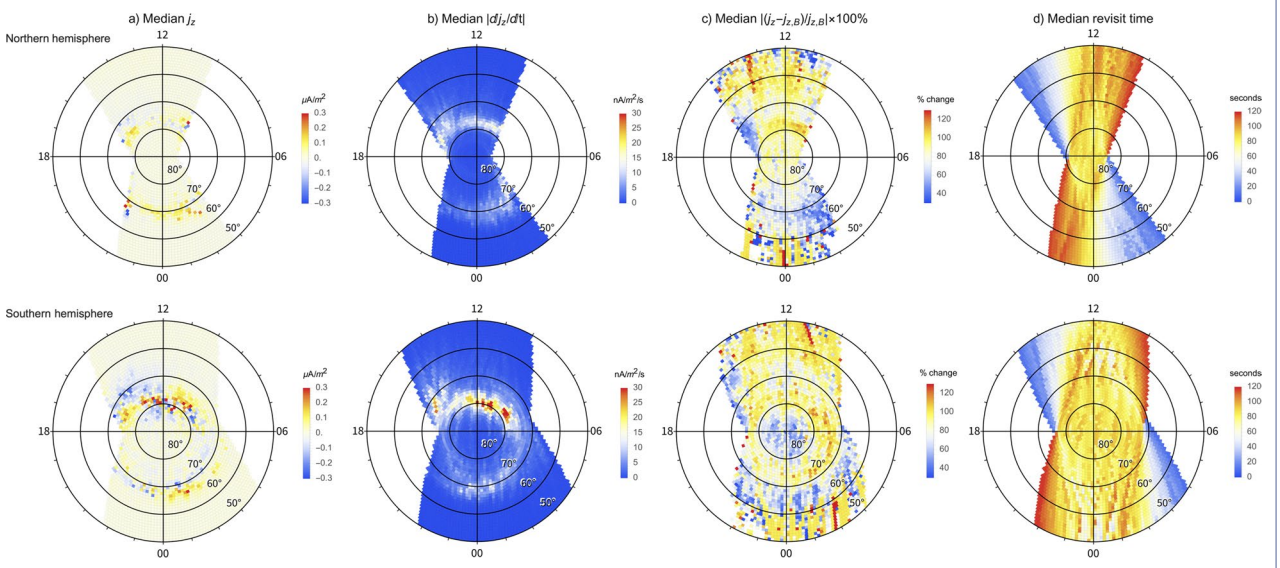

For a moment, nothing happened.

Then, after a second or so, nothing continued to happen.

- Douglas Adams, The Hitchhiker's Guide to the Galaxy.

Space-time ambiguity

Measurements made from an orbiting platform contain artifacts of Doppler-shifted structures that appear as time-varying signals. This represents an ambiguity with respect to underlying temporal variations, whether the time series comes from a single satellite or is derived from a cluster of them (see Dunlop et al. 1988; Balogh et al. 1997).

The quotation above is apropos for an assumption often made to circumvent the space-time ambiguity: that the structure does not change in the time it takes to traverse it. A classic example is the identification of the magnetic field-aligned currents in the polar regions (Birkeland 1908), global patterns of which were characterized half a century ago with magnetic field measurements from the Triad satellite (see Zmuda and Armstrong 1974, and related papers). Contemporary observations reveal variability in these Birkeland currents at large scales on timescales greater than about 10 min (Coxon et al. 2018). Even further variability in the Birkeland currents is evident in their visible manifestation as the Northern and Southern Lights, which can exhibit rapid and dynamic changes in intensity, colour, location and apparent shape. Estimation of current densities using the European Space Agency's Swarm spacecraft (Friis-Christensen et al. 2008) reveal large differences depending on the technique used (Trenchi et al. 2020), some of which variation may be due to violation of the steady-state assumption.

How variable are Birkeland currents on timescales of about a minute or less? A set of two or more closely-spaced satellites moving along a common orbit in a string-of-pearls formation can provide a quantitative answer. Such was approximately the case for the Swarm trio of low-Earth-orbiting satellites in the weeks following their launch on 23 November 2013 by a single rocket into a near-circular, near-polar orbit.

In what follows, I describe a technique for estimating space series and use it to quantify the time variability of the vertical component of electric current density for Swarm crossings of the auroral zones in late November and December 2013. Case study and statistical analysis show that relative changes in Birkeland currents can exceed 100% in less time than it takes a single satellite to cross an auroral zone.

Estimation of space series

A space series is a collection of measurements at different positions made at the same time.[1] The spatial resolution of the series is determined by the ratio of the satellite

[1] Measurements may be deemed simultaneous if they agree to within the timing accuracy, say 10 ms.

speed to the sample rate of the underlying measurements' time series, whereas the time resolution at a given point is determined by the revisit times of the satellites.[2]

Video 1 (Additional file 1) illustrates the relationships between the time series and space series for magnetic field perturbations (with respect to a model field) measured by the three Swarm satellites in a pearls-on-a-string orbital configuration. Grid lines represent along-track distance and time. The gray curves represent the satellites' time series measurements of the perturbations, which were made between 06:24 UTC and 06:36 UTC on 13 December 2013. Swarm B makes its measurement at a given position first, followed by Swarm A about 30 s later and Swarm C about a minute after Swarm A. By interpolating in time between pairs of curves, a space series can be constructed (white curve) at a given time spanning the orbit between the leading satellite and the last trailing satellite. Depending on the time, the estimate at a given position is from an interpolation between measurements made by Swarm B and A or by Swarm A and C. No extrapolation is performed for measurements ahead of the leading satellite or behind the last satellite of the formation such that the space series moves along the orbit as a sliding window. Once a series has been constructed, the along-track component of its spatial gradient can be calculated at a given time using symmetric finite differencing. Gradients at the leading and trailing data points of the series are undefined.

A model is needed to describe how measurements vary between satellite revisit times. The choice here is to interpolate measurements linearly in time. This has the benefit of allowing reconstruction of a space series at arbitrary times. For convenience the time sample rate of a space series is set equal to the instrument sample rate. A second benefit to linear interpolation is that the time derivative of the measurements is easily calculated, it being constant between any pair of satellite visits at a given point along the orbit. Although it is unrealistic to expect measurements to actually vary linearly in time, the result has a useful interpretation: the time derivative represents a lower bound on highest rate at which the measurements could have varied between revisit times.

The sample positions are those of the leading satellite along the orbit, at the so-called along-track distance, which is calculated by setting the distance to zero at the first time and integrating the along-track component of satellite velocity with respect to time. It remains to decide how to represent the positions of the trailing satellites.

[2] A different implementation might interpret an instrument's sample rate another way.

Were each satellite following precisely the same orbit, it would suffice to determine the initial distance lags of the trailing satellites and integrate numerically the satellites' velocities. This method fails to produce sensible results when the orbits are slowly changing, as was the case with Swarm following launch. After many orbits, the satellites have slightly different ephemeres (quasi-dipole latitude, for example) for a given along-track coordinate.

A robust method for determining the positions of the trailing satellites is to assign the along-track distance of the trailing satellites according to their distance from the leading satellite. This takes into account the slightly different orbital elements.

With the along-track positions of each satellite precomputed for a given time interval, the space series are calculated using linear interpolation of measurements made by two satellites at the nearest along-track distance to the requested position at two times. The ephemeres of the series are computed using linear interpolation of the ephemeres of the corresponding satellites in a similar way.

Data analysis

This scheme has been programmed in C for the Swarm string-of-pearls formation. Source code is available on my GitHub account under a GPL license. Docker can get the software up and running quickly on several operating systems. Although the focus here is Birkeland currents, the software can produce space series and statistics for electron density, electron temperature, satellite potential, and ion drift as well.

Magnetic residuals are estimated by subtracting the CHAOS-7 internal magnetic field model (Finlay et al. 2020) from the Swarm high-resolution magnetic field measurements (Jørgensen et al. 2008). Version 7.12 of the CHAOS spherical harmonic coefficients are used. To save time, model fields are calculated along each satellite's orbit at a cadence of one model vector every four seconds, and these are linearly interpolated to the 50 samples-per-second rate of the magnetic field data.

To reduce the amount of computer memory and processing time needed to compute each space series, the magnetic residuals are then downsampled, by averaging, to two vectors per second. Magnetic residuals are transformed into the satellite-track-aligned frame. This frame's unit vectors are defined with respect to the North, East, and Centre (NEC) location and velocity of the satellite as $\hat{x} = \hat{v}_{\text{sat}}$, $\hat{y} \propto \hat{C} \times \hat{x}$, and $\hat{z} = \hat{x} \times \hat{y}$. Vertical current densities are estimated from Ampere's law (ignoring the displacement current) using the along-track gradient of the horizontal cross-track magnetic residual (δB_y), under the assumption that the satellite traverses a one-dimensional current system at normal incidence. The resolution of the

1 Hz Swarm magnetic field measurements is ~ 0.17 nT (Tøffner-Clausen et al. 2016), which corresponds to an uncertainty in the derived 2 Hz current densities of about 0.05 μ A/m^2.

Video 2 (Additional file 2) shows space series and all-sky-imager (ASI) imagery for an overflight of the Swarm trio of the Fort Yukon THEMIS site on 1 December 2013 around 10:40 UTC. The trailing satellite (Swarm C) follows 289 km behind the leading satellite (Swarm B), and the maximum cross-track separation is 10 km at the end of the interval.

The ASI instrument look direction has been calibrated using the locations of up to 20 of the brightest stars in the field of view for each of the 1,200 images over the period 10:00 UTC to 11:00 UTC. The auroral emissions are projected to the mean Swarm altitude of 492 km by tracing magnetic lines of force of the CHAOS−7.12 core and static model fields from an assumed emission altitude of 110 km. Field-line tracing is done using the `gsl_odeiv2_step_msadams` integrator from the GNU Scientific Library (Galassi et al. 2002). It is necessary to ensure accurate calibration of the ASI orientation and accurate field-line tracing. For example, a 0.1° error in look direction of an ASI pixel near zenith corresponds to a horizontal error of approximately 1 km at the projected altitude. The satellite configuration is shown atop the ASI imagery in Video 2 (Additional file 2), along with geographic graticules.

Shown on the left in Video 2 (Additional file 2) are space series for δB_y (top panel), j_z (middle panel) and the THEMIS ASI signal (bottom panel) along the satellite track. Measurement positions are shown on the abscissa in quasi-dipole magnetic latitude (QDLat) and magnetic local time (MLT), as defined in Emmert et al. (2010). The gray solid curve in each panel is the apparent space series obtained from assuming a steady-state system, shown for the Swarm B (leading satellite) measurements. The thick white curve in each panel shows estimated space series at the displayed time. Displacements of the trailing satellites relative to the leading satellite are shown. The x and y coordinates represent the along-track and horizontal cross-track displacements. The z coordinate represents the difference in altitudes of the satellite pairs. Shown also are maximum-absolute and root-mean-square differences, which represent lower bounds of the error in the static assumption with respect to the space series estimates at each time step.

The ASI signal for the steady-state assumption is representative of a profile for a satellite-aligned keogram (see Gillies et al. 2015). ASI image processing consists first of estimating a background image constructed from the minimum pixel value for each pixel over the interval from 14:00 UTC to 15:00 UTC, a period when very little auroral signal is present. This image is subtracted from each offset-corrected level 1 ASI image. To improve signal-to-noise, the mean of the 5 nearest pixels at each point along the satellite track is plotted.

The example in Video 2 (Additional file 2) corresponds to a visually quiescent auroral arc exhibiting no obvious cross-track spatial variation. The upward current density near the peak of the auroral emission is consistent for all three satellites. There are notable differences between the static assumption for Swarm B and the dynamic space series poleward of the brightest arc, in particular associated with possible along-track motion of the narrow, intense downward current system as the last satellite approaches the arc. This is suggestive of the Alfvénic aurora (e.g., Chaston et al. 2008).

Figure 1 provides a zoom on the space and time series from Video 2 (Additional file 2) at a time (10:41:44.5 UTC) when Swarm A (whose position is denoted by the vertical dotted line in the middle panel) observes a downward current density of ~ 1.0 μ A/m^2. This was observed 13.7 s following Swarm B's observation of a ~ 0.3 μ A/m^2 upward current density. The two measurements are within a cross-track distance of 3 km.

Video 3 (Additional file 3) shows space series and ASI imagery for an overflight of the Swarm trio of the Rankin Inlet THEMIS site on 25 December 2013 around 05:20 UTC. The frame format is similar to that shown in Video 2 (Additional file 2). The ASI imagery is shown projected at the mean Swarm altitude of 497 km by tracing CHAOS−7.12 model field lines from an assumed emission altitude of 150 km, an altitude for which the ASI signal peaks appear to line up slightly better with the positive vertical current density peaks than for an emission altitude of 110 km. A perfect alignment between these signals is not expected, largely due to the way narrow sheets of auroral emission appear to span latitude for off-zenith look directions.

The aurora shown in Video 3 (Additional file 3) is highly structured in both time and space. In this example, more than three weeks after the one shown in Video 2 (Additional file 2), Swarm C trails Swarm B by ~ 1083 km, and their cross-track separation exceeds 45 km at the end of the interval. Some of the error between the static assumption and the space series can be attributed to horizontal cross-track structure associated with the mis-alignment of the satellite orbits. Estimation of time derivatives are less reliable in this case. The sequence of rising square-wave features equatorward of 70° QDLat results from a flashing light near the southern horizon. The intense, narrow spike on the equatorward side of the main auroral emissions between 05:23:00 UTC and 05:23:40 UTC is starlight. This spike does not appear for projections of imagery corresponding to an emission

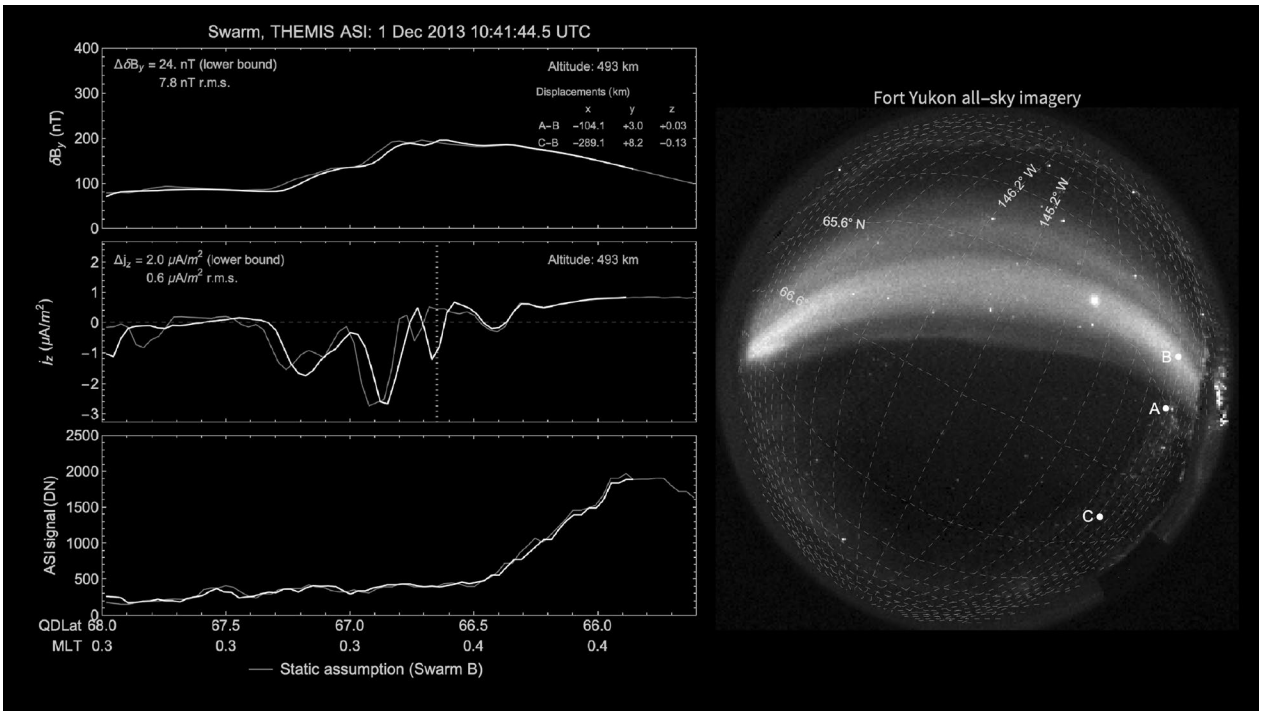

Fig. 1 Space series and all-sky imagery from a Swarm overflight of the Fort Yukon THEMIS site on 1 December 2013 at 10:42:01 UTC. The dashed line in the middle panel marks where Swarm A measured a downward current density of $\sim 1.0\ \mu$ A/m^2 about 14 s after Swarm B measured an upward current density of $\sim 0.3\ \mu$ A/m^2

altitude of 110 km, incidating that uncertainty in the average emission altitude of each pixel contributes significantly to errors in comparisons of satellite measurements with imagery. In any case, the auroral imagery provides validation of the upward vertical current density shown in the space series. This example demonstrates the importance of precise orbit control in the design of multi-satellite missions for estimating space series of auroral and ionospheric parameters.

Statistics of Birkeland current variability

Space series are calculated here for intervals of 24 h from midnight to midnight. Due to satellite commissioning activities, several days in late November and early December 2013 have full operations of the vector field magnetometers for only two satellites. Space series derived from these two-satellite cases and the remaining three-satellite cases between 25 November and 31 December 2013 are included in the statistical results below. Data from 13 December 2013 have been excluded owing to the presence of a large number of artifacts in the results. Data from 1 January 2014 and later are not included, by which time the along-track and horizontal cross-track separations of the satellites are quite large and continue to grow.

Statistical binning in QDLat and MLT is done on a grid of approximately "equal-area" bins. The bin size is defined as one third of the solid angle of a polar cap spanning quasi-dipole latitude from 89° to 90°. To reduce the influence of outliers on the results, statistics are estimated using the median as implemented in the GNU Scientific Library (Galassi et al. 2002).

Results are illustrated in Fig. 2. The panels in the top row represent results for the northern hemisphere, and the panels in the bottom row represent results for the southern hemisphere. The left-hand column (a) shows median vertical current densities j_z in units of μ A/m^2. Despite the short time interval of just over 1 month, there are clear indications of the region 1 and region 2 current systems of Iijima and Potemra (1978). This validates the use of the vertical component of electric current density as a proxy for Birkeland (magnetic-field-aligned) currents at high latitudes. In the vicinity of the auroral oval, the median magnitudes are of order a few tenths of a microampere per square meter. The magnitudes are greater in the summer (southern) hemisphere than in the winter (northern) hemisphere.

The second column (b) of Fig. 2 shows the per-bin median of the magnitude of the time derivative of the vertical current density. Rates of change peak between

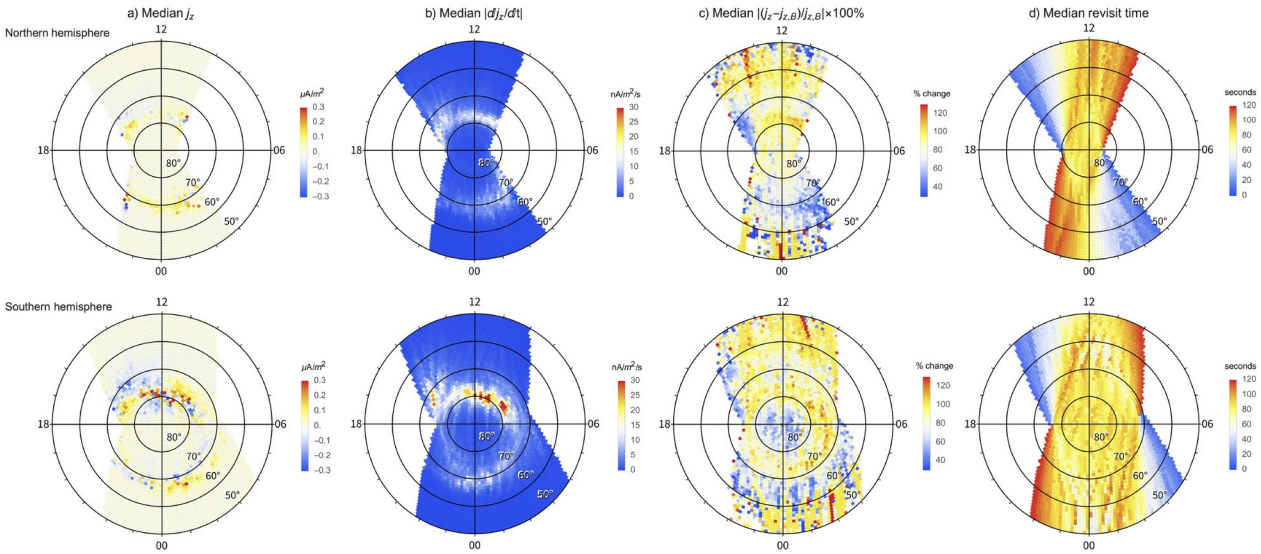

Fig. 2 **a** Median statistics of j_z represented in equal-area bins of quasi-dipole latitude and magnetic local time for the northern hemisphere (top panel) and southern hemisphere (bottom panel) from 25 November 2013 to 31 December 2013. **b** Median statistics of the magnitude of the time-rate-of-change of j_z. **c** Median of the magnitude of the percentage change in current density relative to the Swarm B static assumption. **d** Median statistics of the trailing satellites' revisit times with respect to the measurement times of the leading satellite

5 $\mathrm{nA/m^2/s}$ and 15 $\mathrm{nA/m^2/s}$ in the northern hemisphere, and exceed 30 $\mathrm{nA/m^2/s}$ in the southern hemisphere. The currents are more variable on the dayside in a region morphologically similar to the magnetic cusp-cleft.

To illustrate the extent to which the static assumption is violated during auroral zone crossings, the per-bin median of the magnitude of the percentage change in current density relative to the static assumption calculated from Swarm B measurements ($|j_z - j_{z,\mathrm{B}}|/j_{z,\mathrm{B}} \times 100\%$) is shown in the third column (c) of Fig. 2. To avoid excessively large percentage changes associated with small $j_{z,\mathrm{B}}$ in the denomenator, only those measurements for which the Swarm B current density magnitude is at least 0.05 μ $\mathrm{A/m^2}$ are retained in the statistics. The orientation of the Swarm orbits is such that in the northern hemisphere the satellites move from day-side to night-side, whereas in the southern hemisphere they move from night-side to day-side. The orbits precess slowly with a tendency for post-noon and post-midnight local times in late November and pre-noon and pre-midnight local times in late December. An increase in errors from post-noon to pre-noon in the northern dayside auroral zone likely has a significant contribution associated with the increasing along-track satellite separations as time goes on. For reference, the median revisit time of the trailing satellites with respect to measurements made by the leading satellite is shown in the right-hand column (d) of Fig. 2. This shows that the space series technique as applied to the Swarm data obtains samples, in effect, corresponding to periods spanning from a few seconds (shortly after launch) to about 2 min (near the end of 2013).

It is a limitation of the technique as implemented for Swarm (but not generally, to the extent that satellite orbits are precisely controlled for this purpose) that horizontal gradients are assumed to be zero. Yet the variation in satellite separation does not appear to affect significantly the time derivative shown in the middle column of Fig. 2, which shows large values both post-noon and pre-noon yet smaller values pre-midnight than post-midnight. This indicates that errors in current density (right-hand column of Fig. 2) associated with assuming no horizontal cross-track spatial gradients are typically smaller than errors associated with the static assumption.

Closing remarks

Swarm early mission magnetic field data (Fig. 2 columns c and d) reveal that single satellite estimates of Birkeland currents can be erroneous by tens of percent within 10 s of the measurement and by up to 100% within one to two minutes. Accurate determination of time derivatives potentially has implications for investigations of Alfvén waves, Poynting flux, ionospheric conductance, and auroral structure.

Linear time interpolation is not robust against aliasing, and it does not capture correctly the time variation associated with along-track drift of spatial structures. Neither does it account for cross-track drift of structures with cross-track gradients. These issues point to the need for

large numbers of closely-spaced orbital platforms in two and three dimensions to fully characterize space and time variability and to capture the time history of the system (see Burleigh et al. 2022).

Obtaining massively parallel measurements from fleets of relatively inexpensive cubesats capable of orbit control is a feasible approach. Such missions need to be designed with the capability to maintain precise control of orbital parameters. Accurate measurement of cross-track and along-track ion drift could help to estimate partial time derivatives in a frame of reference moving with the plasma, rather than the total time derivatives along the orbit as estimated here. In terms of measuring Birkeland currents, one imagines multi-cluster missions consisting of small groups of spacecraft capable of measuring $\nabla \times \mathbf{B}$ at many points along a trajectory simultaneously to resolve space-time ambiguity during a traversal of the current system. Such capability would enable measuring space series of the vector current density, rather than just the vertical component of it.

The gradually increasing separation of the Swarm satellites following launch was orchestrated to support observations of east–west magnetic field gradients associated with crustal magnetism. After several months of orbital maneouvres, Swarm A and C were closely spaced near an altitude of ~ 460 km separated by 1.4° of longitude, with Swarm C leading Swarm A by 4 s to 10 s throughout the mission. (Swarm B was placed at an altitude of ~ 510 km, its orbital plane precessing slowly with respect to those of the lower pair.) In the vicinity of the geographic poles, Swarm A and C have small cross-track separations. This suggests an opportunity for using space series to study the morphology of fine-scale variability of Birkeland currents and other ionospheric parameters with a long-term dataset. The larger offset of the magnetic and geographic poles in the southern hemisphere should provide sufficient coverage of magnetic latitude and local time to cover significant portions of the auroral oval. This would have application in filtering high-latitude magnetic field measurements used in global field models (e.g., Finlay et al. 2020).

Abbreviations

ASI	All-sky imager
ESA	European Space Agency
MLT	Magnetic local time
NEC	North, east, centre reference frame
QDLat	Quasi-dipole magnetic latitude
UTC	Universal time coordinated

Supplementary Information

The online version contains supplementary material available at https://doi.org/10.1186/s40623-023-01867-8.

Additional file 1: Video S1. Animation of the measurements of magnetic field perturbations (gray curves) from three Swarm satellites in a pearls-on-a-string orbital configuration, as well as the time development of the space series (white curve) interpolated in time from those measurements.

Additional file 2: Video S2. Space series of δB_y, j_z, and ASI signal during a Swarm overflight of the Fort Yukon THEMIS all-sky imager on 1 December 2013 around 10:40 UTC.

Additional file 3: Video S3. Space series of δB_y, j_z, and ASI signal during a Swarm overflight of the Rankin Inlet THEMIS all-sky imager on 25 December 2013 around 05:20 UTC.

Acknowledgements
The author thanks David Knudsen for financial support. Megan Gillies from the University of Calgary Auroral Imaging Group provided technical advice on THEMIS ASI calibrations. The Swarm-Aurora conjunction finder (https://swarm-aurora.com) was used to find the events shown in Video 2 (Additional file 2) and Video 3 (Additional file 3). The author is grateful to two anonymous reviewers for their insightful critiques of the manuscript.

Author contributions
JKB thought of the idea, developed the source code, analyzed the data, made the visualizations, interpreted the results, and wrote the paper.

Funding
This study was carried out with financial support from the Canadian Space Agency.

Availability of data and materials
Swarm data are available from http://swarm-diss.eo.esa.int. THEMIS ASI level 1 and 2 data are availble from http://themis.ssl.berkeley.edu/data/themis/thg/. ASI calibration was carried out using https://github.com/JohnathanBurchill/AllSkyCameraCal. Swarm magnetic field residuals and CHAOS-7 model field-line tracing were computed using https://github.com/JohnathanBurchill/chaos. Quasi-dipole magnetic coordinates were calculated using https://github.com/JohnathanBurchill/QuasiDipole. Swarm space series were calculated using https://github.com/JohnathanBurchill/spaceseries.

Declarations

Competing interests
The author declares to have no competing interests.

Author details
[1]Department of Physics and Astronomy, University of Calgary, Calgary, Canada.

Received: 4 March 2023 Accepted: 30 June 2023
Published online: 21 July 2023

References

Balogh A, Dunlop M, Cowley S, Southwood D, Thomlinson J, Glassmeier K, Musmann G, Lühr H, Buchert S, Acuna M et al (1997) The cluster magnetic field investigation. Space Sci Rev 79(1):65–91

Birkeland K (1908) On the cause of magnetic storms and the origin of terrestrial magnetism, vol 1. H. Aschehoug, Oslo

Burleigh M, Lynch K, Zettergren M, Clayton R (2022) Spatiotemporal limitations of data-driven modeling: an isinglass case study. J Geophys Res Space Phys 127(9):e2021JA030242

Chaston C, Salem C, Bonnell J, Carlson C, Ergun R, Strangeway R, McFadden JP (2008) The turbulent alfvénic aurora. Phys Rev Lett 100(17):175003

Coxon JC, Milan SE, Anderson BJ (2018) A review of Birkeland current research using ampere. Electr Curr Geosp Beyond. https://doi.org/10.1002/9781119324522.ch16

Dunlop M, Southwood D, Glassmeier KH, Neubauer F (1988) Analysis of multipoint magnetometer data. Adv Space Res 8(9–10):273–277

Emmert J, Richmond A, Drob D (2010) A computationally compact representation of magnetic-apex and quasi-dipole coordinates with smooth base vectors. J Geophys Res Space Phys. https://doi.org/10.1029/2010JA015326

Finlay CC, Kloss C, Olsen N, Hammer MD, Tøffner-Clausen L, Grayver A, Kuvshinov A (2020) The chaos-7 geomagnetic field model and observed changes in the south atlantic anomaly. Earth Planets Space 72(1):1–31. https://doi.org/10.1186/s40623-020-01252-9

Friis-Christensen E, Lühr H, Knudsen D, Haagmans R (2008) Swarm-an earth observation mission investigating geospace. Adv Space Res 41(1):210–216

Galassi M, Davies J, Theiler J, Gough B, Jungman G, Alken P, Booth M, Rossi F, Ulerich R (2002) GNU scientific library. Network Theory Limited Godalming

Gillies DM, Knudsen D, Spanswick E, Donovan E, Burchill J, Patrick M (2015) Swarm observations of field-aligned currents associated with pulsating auroral patches. J Geophys Res Space Phys 120(11):9484–9499

Iijima T, Potemra TA (1978) Large-scale characteristics of field-aligned currents associated with substorms. J Geophys Res Space Phys 83(A2):599–615

Jørgensen JL, Friis-Christensen E, Brauer P, Primdahl F, Jørgensen PS, Allin TH, Denver T et al (2008) Small satellites for earth observation. In: Valenzuela A (ed) The swarm magnetometry package. Springer, Dordrecht, pp 143–151

Tøffner-Clausen L, Lesur V, Olsen N, Finlay CC (2016) In-flight scalar calibration and characterisation of the swarm magnetometry package. Earth Planets Space 68:1–13. https://doi.org/10.1186/s40623-016-0501-6

Trenchi L, Team FM, Kauristie K, Käki S, Vanhamäki H, Juusola L, Blagau A, Vogt J, Marghitu O, Dunlop M, et al (2020) ESA field-aligned currents–methodology inter-comparison exercise. In: MW Dunlop, H Lühr (eds.) Ionospheric Multi-Spacecraft Analysis Tools Approaches for Deriving Ionospheric Parameters. Frascati, European Space Agency, pp 167–188

Zmuda AJ, Armstrong JC (1974) The diurnal flow pattern of field-aligned currents. J Geophys Res 79(31):4611–4619

Publisher's Note